

Strong charge fluctuations manifested in the high-temperature Hall coefficient of high- T_c cuprates

S. Ono, Seiki Komiya, and Yoichi Ando*

Central Research Institute of Electric Power Industry, Komae, Tokyo 201-8511, Japan

(Dated: May 25, 2019)

By measuring the Hall coefficient R_H up to 1000 K in La_2CuO_4 , $\text{Pr}_{1.3}\text{La}_{0.7}\text{CuO}_4$, and $\text{La}_{2-x}\text{Sr}_x\text{CuO}_4$ (LSCO), we found that the temperature (T) dependence of R_H in LSCO for $x = 0 - 0.05$ at high temperature undoubtedly signifies a gap over which the charge carriers are thermally activated, which in turn indicates that in lightly-doped cuprates strong charge fluctuations are present at high temperature and the carrier number is not a constant. At higher doping ($x = 0.08 - 0.21$), the high-temperature $R_H(T)$ behavior is found to be qualitatively the same, albeit with a weakened temperature dependence, and we attempt to understand its behavior in terms of a phenomenological two-carrier model where the thermal activation is considered for one of the two species. Despite the crude nature of the model, our analysis gives a reasonable account of R_H both at high temperature and at 0 K for a wide range of doping, suggesting that charge fluctuations over a gap remain important at high temperature in LSCO deep into the superconducting doping regime. Moreover, our model gives a perspective to understand the seemingly contradicting high-temperature behavior of R_H and the in-plane resistivity near optimum doping in a consistent manner. Finally, we discuss possible implications of our results on such issues as the scattering-time separation and the large pseudogap.

PACS numbers: PACS numbers: 74.25.Fy, 74.72.-h, 74.72.Dn

I. INTRODUCTION

The Hall coefficient R_H is generally a useful tool to characterize metals and semiconductors, for it reflects the band structure and the sign of charge carriers. In strongly-correlated electron materials, R_H often shows complex dependences on temperature and other control parameters, which are expected to give a clue to understanding the underlying unconventional electronic states; in this context, R_H has been used for the studies of such novel phenomena as quantum phase transition^{1,2,3,4} or charge-stripe formation.⁵ Nevertheless, quantitative understandings of R_H in strongly-correlated electron materials have been difficult to achieve, and high- T_c cuprate superconductors are no exception.⁶ In fact, since the optimally-doped cuprates are just in the middle of the strong- and weak-coupling limits,^{6,7} even the basic framework for the description of its electronic state is still controversial; as a result, most of the normal-state transport properties, including the Hall coefficient, are generally believed to be too complicated to be quantitatively understood, though there have been attempts to explain their fundamental behavior in frameworks of specific theories.^{8,9,10,11}

In this context, however, the R_H of high- T_c cuprates appears to be rather peculiar, because in the lightly hole-doped regime where the low-energy physics is apparently governed by the “Fermi arc” (a small portion of the large Fermi surface expected in the absence of electron correlations),^{6,12} we have recently found¹³ that R_H simply behaves like the “Hall constant” of a conventional metal and the electron correlation effects seem to be implemented only through modifications of the Fermi surface in determining R_H . This finding in cuprates suggests

that R_H might give us a unique opportunity to find a clue to building a proper framework for the description of the electronic state of cuprates despite the strong electron correlations. It should be emphasized that there is still no proper theoretical understanding for *how* the correlation gap is suppressed (and eventually closed) when carriers are doped to a Mott insulator, so any new information regarding the band structure of doped Mott insulators (to which cuprates belong) would be of fundamental importance for addressing the strong electron correlation problem.

The $\text{La}_{2-x}\text{Sr}_x\text{CuO}_4$ system¹⁴ we study here is a prototypical cuprate, where $x = 0$ is a parent charge-transfer (CT) insulator^{12,15,16} with the band gap Δ_{CT} called the CT gap. We also study another parent CT insulator $\text{Pr}_{1.3}\text{La}_{0.7}\text{CuO}_4$ (PLCO) for comparison. In our previous work,¹³ besides showing that R_H of LSCO at low doping can be interpreted as a “Hall constant” below 300 K, we reported that a marked decrease sets in at higher temperature, which was proposed to be possibly due to the contribution of thermally-created holes. In the present work, in an effort to quantitatively understand the temperature dependence and the doping evolution of R_H in LSCO and to elucidate the electronic structure of this system, we have extended the high-temperature measurements of $R_H(T)$ to a wide doping range, starting from $x = 0$. As a result, we find that the behavior of $R_H(T)$ at $x = 0$ is surprisingly well understood in the framework of conventional semiconductor physics, and furthermore our data in the lightly-doped region are found to give a solid basis for understanding the high-temperature behavior in terms of the thermal activation of charge carriers over a well-defined gap. At higher doping, the behavior of $R_H(T)$ becomes less unambiguous to understand, and in

this paper we present our attempt to describe its behavior in terms of a phenomenological two-carrier model.

II. EXPERIMENTAL

The $\text{La}_{2-x}\text{Sr}_x\text{CuO}_4$ and $\text{Pr}_{1.3}\text{La}_{0.7}\text{CuO}_4$ single crystals are grown by the traveling-solvent floating-zone method. The LSCO crystals are annealed to tune the oxygen content to 4.000 ± 0.001 as described in Refs. 17 and 18. In particular, the oxygen stoichiometry of the $x = 0$ samples (which are annealed in flowing Ar at 800°C) is confirmed by both the thermo-gravimetry analysis and the magnetic susceptibility, which shows a very sharp Néel transition at 321 K. The x values shown here are determined by the inductively-coupled-plasma atomic-emission-spectroscopy analysis. The PLCO crystals are annealed in flowing O_2 at 700°C to minimize oxygen deficiency. To measure R_H at temperatures up to 1000 K, we use a 6-T superconducting magnet system with a room-temperature bore, in which a water-cooled furnace is fit. Samples are kept under suitable atmospheres during the experiments to ensure that the oxygen content does not change. For the measurements of R_H using a standard six-probe technique, we record the full magnetic-field dependence of the Hall voltage at a fixed temperature by sweeping the magnetic field to both plus and minus polarities, subtract the asymmetric part coming from contact misalignment, and fit the symmetrical part with a straight line to determine R_H , which is essential for the high accuracy achieved in the present work.

Because the present work involves transport measurements in temperatures up to 1000 K which is much higher than usual, it would be prudent to discuss the possibility that the high-temperature Hall data might be adversely affected by the oxygen mobility within a sample or by some change in the oxygen content: As for the oxygen mobility at high temperature, this can in principle provide a parallel channel for charge transport; such an effect is actually important in a mixed ionic and electronic conductors such as $\text{GdBaMn}_2\text{O}_{5+x}$ which was recently found to have a very high oxygen mobility,¹⁹ but in LSCO the oxygen-ion conductivity at 1000 K is negligible compared to the electron conductivity. Of more concern might be that the moving oxygen could affect the electron transport in an unexpected way; however, this is very unlikely to be the case in LSCO, because the oxygen diffusion time at 1000 K is of the order of 10^{-8} s, while the electron scattering time is of the order of 10^{-13} s at best, so the electrons only see static oxygen environment during the transport events. Regarding the oxygen content issue, it should be emphasized that in the present experiment the atmosphere in the furnace is optimized for different doping ranges to minimize the change in the oxygen content in the samples during the measurements. For example, in the lightly-doped region of LSCO one should only worry about excess oxygen, so the measurements are done in pure argon; on the other hand, in the optimally- to over-

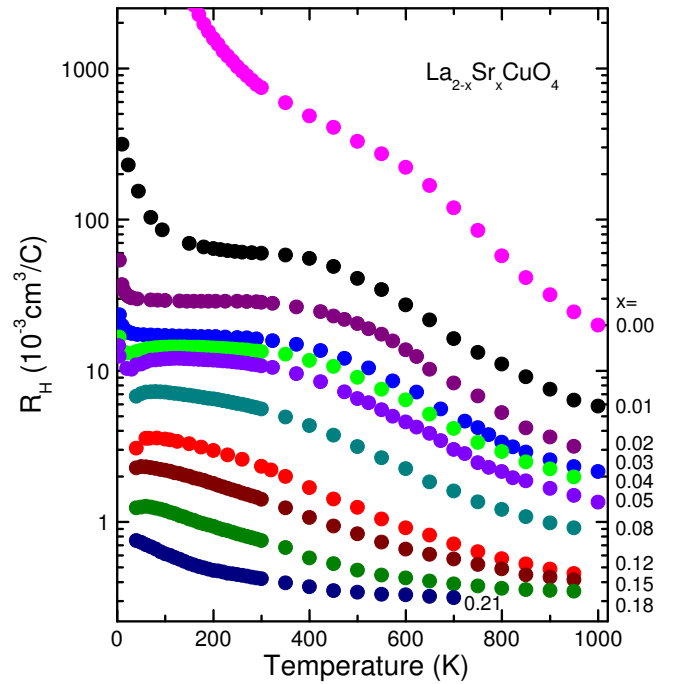


FIG. 1: (color online) Temperature dependences of R_H up to 1000 K measured on a series of high-quality LSCO single crystals.

doped region one should worry about oxygen vacancies rather than excess oxygen, so the measurements are done in 1 atm of oxygen. (Since we cannot avoid noticeable oxygen loss at high temperature for $x > 0.20$, we show data only up to 700 K for $x = 0.21$ in this work.) Since the oxygen phase diagram is known for the whole range of Sr doping for LSCO,²⁰ we can be sure that the possible change in the effective hole doping is less than 1% during the measurements up to 1000 K under our measurement conditions.

III. RESULTS

Figure 1 shows the $R_H(T)$ data of LSCO single crystals up to 1000 K for the whole doping range studied. Those data are essentially consistent with the previously-reported high-temperature data measured on polycrystalline samples,^{21,22} but bear much higher accuracies. Note that there has been no high-temperature data for $x = 0 - 0.03$ even for polycrystalline samples, and it turns out that the data from this insulating regime provide important insights for analyzing the data for higher dopings. In the following, we describe our analyses of the data, starting from the parent insulator, $x = 0$.

A. Parent Insulators

Interestingly, the temperature dependence of R_H is found to be most unambiguously understood in the parent CT insulator La_2CuO_4 , where the electron correlation effects are the strongest; Fig. 2(a) shows the $R_H(T)$ data up to 1000 K together with the fitting to the formula,

$$R_H(T) = \frac{V_{Cu}}{e} \left(n_0 e^{-\Delta_{imp}/2k_B T} + n_1 e^{-\Delta_{CT}/2k_B T} \right)^{-1}. \quad (1)$$

It is clear in Fig. 2(a) that this fitting is essentially perfect, which means that $R_H(T)$ at $x = 0$ is simply governed by two gaps (e is the electron charge and V_{Cu} is the unit volume per Cu). The lower-temperature part of the data tells us that there is a small concentration ($n_0 = 0.57\%$) of impurity states located at $\Delta_{imp} = 0.087$ eV above the top of the valence band; such a situation has been already known¹⁴ for La_2CuO_4 , where Δ_{imp} determines the impurity-ionization energy.²³ What is new here is that at high temperature above ~ 500 K another activation process with $\Delta_{CT} = 0.89$ eV involving a large density of states becomes active, which obviously corresponds to the activation across the CT gap. A schematic energy diagram is shown in the inset of Fig. 2(a). The fact that R_H is positive at high temperature means that the holes in the valence band are more mobile than the electrons in the conduction band; indeed, if one remembers¹⁶ that the valence band in cuprates is primarily of O 2p character (implying a wide band), while the conduction band is essentially a Cu 3d band (which is always narrow²⁴), it is reasonable for the holes to have higher mobility and become dominant. Our fitting yields the prefactor of the high-temperature excitation term, n_1 , of as large as 4.3 hole/Cu; although this exceeds the logical limit of 1 hole/Cu, this is actually reasonable because the contribution of the electrons (that are created with holes) tends to reduce the R_H value and lead to an increase²⁴ in the effective n_1 .²⁵ In any case, n_1 being larger than 1 hole/Cu strongly suggests that we are observing excitations across major bands.

Figure 2(b) shows similar data for PLCO, which has the so-called T' structure¹⁵ and is the parent insulator for an electron-doped material. The sign of R_H is negative below 700 K, which indicates that the impurity states (that are presumably due to some oxygen nonstoichiometry) lie close to the conduction band and provides electron carriers at moderate temperature. However, R_H of PLCO shows a sign change above 700 K, corroborating the conclusion obtained for La_2CuO_4 that at high temperature the activation across the CT gap becomes relevant and the hole carriers govern R_H due to their higher mobility.

We note that our Δ_{CT} obtained for La_2CuO_4 gives the thermodynamically measured CT gap, and this is to be compared with the optically measured CT gap,^{12,14} which is usually believed to be about 2 eV. Here, a little caution is needed, because it is customary to take

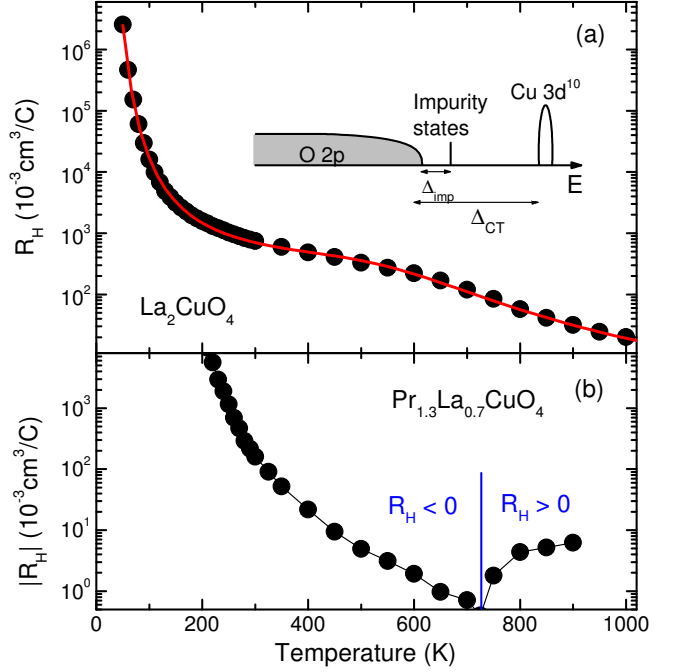


FIG. 2: (color online) (a) R_H of La_2CuO_4 measured up to 1000 K. The solid line is the fit to the data with Eq. (1) with the parameters $n_0 = 0.0057$, $\Delta_{imp} = 0.087$ eV, $n_1 = 4.3$, and $\Delta_{CT} = 0.89$ eV. The inset shows a schematic energy diagram for the relevant bands and states. (b) Absolute value of R_H of $\text{Pr}_{1.3}\text{La}_{0.7}\text{CuO}_4$, which shows a sign change near 700 K.

the *peak energy* of the optical absorption as a measure of the CT gap, but this energy does *not* correspond to the true gap that is best measured as the minimum excitation energy between the two bands and is equal to the distance between the two band edges. When we take the onset of the optical absorption as a measure of the CT gap, the existing optical data¹⁴ give values of 0.9 – 1.3 eV, which is still a bit larger than our thermodynamic value of 0.89 eV. An obvious reason for this difference is that the CT gap is an indirect one,²⁶ but additionally our Δ_{CT} is measured at high temperature, where the weakening of the antiferromagnetic correlations and the band broadening would also reduce Δ_{CT} . Furthermore, polaron effects are likely to be important in insulating cuprates,^{14,27} and these effects would naturally reduce the gap at high temperature.¹⁴ Hence, one may conclude that the CT gap manifested in the Hall effect at $x = 0$ is fully consistent with the optics data.

B. Lightly-Doped Region

Now that $R_H(T)$ of La_2CuO_4 is quantitatively understood, let us see how we can extend this understanding to the lightly-doped region. Figure 3(a) shows the $R_H(T)$ data of LSCO for $x = 0.01 – 0.05$ in a semi-log plot, where R_H [cm³/C] is converted into the inverse of effective carrier number per Cu, $1/n_{\text{eff}}$ ($= eR_H/V_{Cu}$, which is nondi-

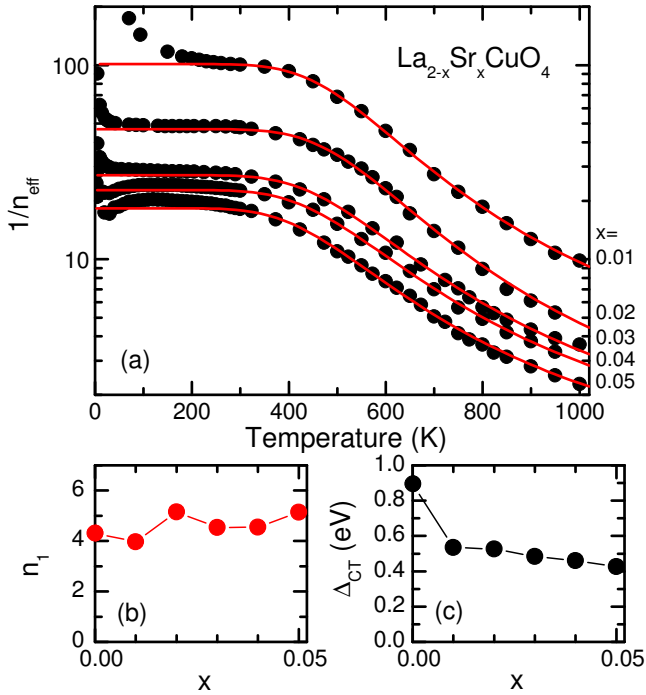


FIG. 3: (color online) (a) T dependences of $1/n_{\text{eff}}$ ($= eR_H/V_{Cu}$) for a series of LSCO single crystals in the lightly-doped region, $x = 0.01 - 0.05$, with their fits (solid lines) using Eq. (2). The fitting parameters, n_1 and Δ_{CT} , are shown in panels (b) and (c).

dimensional), for the ease of understanding the meaning of the numbers. Since the plateau in $R_H(T)$ at moderate temperature gives n_{eff} that is essentially equal to x at low doping,¹³ the impurity term $n_0 e^{-\Delta_{\text{imp}}/2k_B T}$ in Eq. (1) should be replaced with x to describe $R_H(T)$ in this region. Hence, we fit the data for $x = 0.01 - 0.05$ to

$$R_H(T) = \frac{V_{Cu}}{e} \left(x + n_1 e^{-\Delta_{CT}/2k_B T} \right)^{-1}. \quad (2)$$

The solid lines in Fig. 3(a) are the results of the fittings.²⁸ Note that the upturn at very low temperature seen in all the data is due to the strong Anderson localization¹³ that reduces the number of mobile carriers and naturally causes a deviation from Eq. (2). Obviously, Eq. (2) gives a reasonable account of the essential feature of the data (except for the Anderson localization), and hence one may conclude that the thermal activation of holes gives rise to the exponential decrease in R_H at high temperature not only at $x = 0$ but also at low doping. This in turn indicates that there are strong charge fluctuations in lightly-doped cuprates at $\gtrsim 400$ K, where the charge transport must become incoherent; therefore, it is probably not reasonable to describe R_H in this regime using theories developed for a metallic system (i.e., for coherent electrons with well-defined wave vectors), such as that in Ref. 10.

The doping dependences of the parameters n_1 and Δ_{CT} in Eq. (2) obtained from the fits are shown in

Figs. 3(b) and 3(c). It is notable that n_1 , a rough measure of the number of available states for thermal activations (but is amplified by various additional effects^{24,25}) is essentially doping-independent for $x = 0 - 0.05$ [Fig. 3(b)], which would imply that thermal creations of carriers of essentially the same nature are taking place in this doping range. On the other hand, the gap Δ_{CT} for the thermal activation [Fig. 3(c)] shows a sudden drop from 0.89 to 0.53 eV upon doping only 1% of holes to the parent insulator, but then shows only a small decrease with x . Probably, there are two possibilities to interpret this result. One is to take the reduction in Δ_{CT} to be a result of the softening of the main CT gap upon slight doping; in this case, the same bands are involved in the activation process after the doping, and our observation that n_1 is essentially doping independent is in good accord. Considering the fact that doping to a Mott insulator necessarily involves a change in the electronic structure at a high energy scale of the order of the on-site repulsion U (because doping one hole to a Mott insulator not only creates a hole state but also removes one state from the upper Hubbard band),²⁹ it would be possible that a slight doping induces a relatively large change in the band structure. The other possibility is that the so-called “in-gap states”¹² are created in the middle of the original CT gap upon hole doping and our Δ_{CT} actually measures the charge-transfer excitations from these new states to the upper Hubbard band (conduction band). In this case, one would expect n_1 for $x \geq 0.01$ to be much smaller than that for $x = 0$; however, a large n_1 might be possible for some particular shape of the band edge,³⁰ so our result in Fig. 3(b) cannot conclusively exclude this possibility. In any case, the true nature of Δ_{CT} in the doped system is best left as an open question, and its identification is actually at the heart of understanding what really happens upon doping to a Mott insulator. It is intriguing to note that our Δ_{CT} for the lightly-doped region coincides rather well with the peak frequency of the mid-infrared (MIR) absorption seen in the optical conductivity of LSCO,³¹ so the MIR absorption may also have something to do with the CT excitations.

In passing, previous studies of the doping dependence of the CT gap using high-energy probes^{32,33} have found a hardening of the gap, which appears to be at odds with the first possibility discussed above. However, Markiewicz and Bansil argued²⁶ that those high-energy experiments may only see hard branches of the various modes of the CT excitations; naturally, our thermodynamic measurement probes the CT excitation of the lowest energy, which may not be easily seen by the high-energy probes. In this regard, it should be noted that our Δ_{CT} measures the effective excitation energy *at high temperature*, which is naturally smaller than the band gap at $T = 0$, so a care must be taken when comparing our Δ_{CT} to that calculated theoretically for $T = 0$.

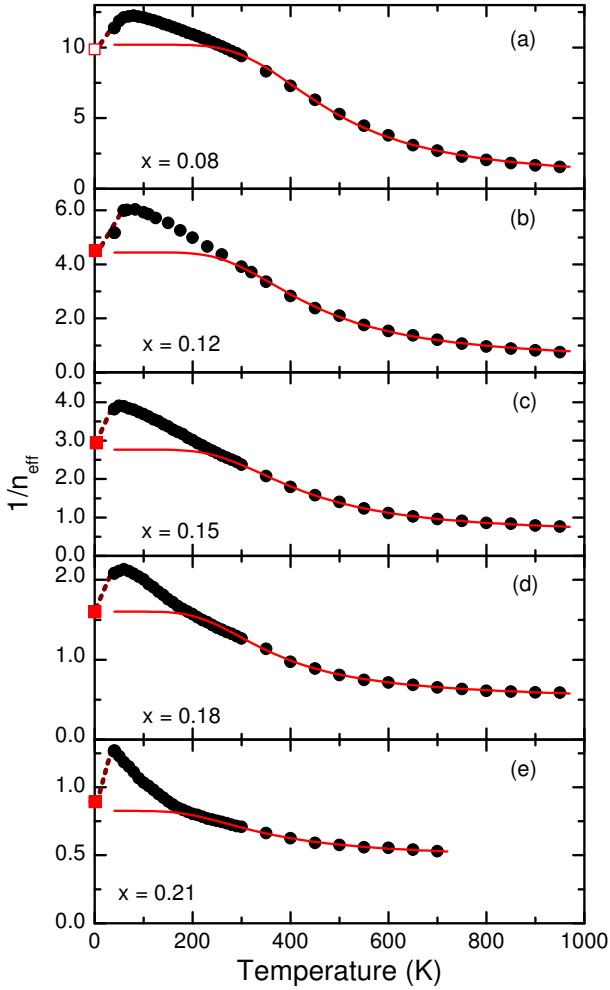


FIG. 4: (color online) The $R_H(T)$ data, converted into the nondimensional $1/n_{\text{eff}}$, for $x = 0.08 - 0.21$ and their fits (solid lines) using Eq. (4). The squares at $T = 0$ mark $R_H(0)$ obtained from the pulsed magnetic-field experiments;⁴³ the $R_H(0)$ value for $x = 0.08$ is obtained by extrapolating the data in Ref. 43 for $10 - 40$ K to $T \rightarrow 0$. The dashed lines are guides to the eyes.

C. Superconducting Doping Range

At higher doping $x \geq 0.08$, Eq. (2) becomes obviously inappropriate, because n_{eff} at moderate temperature is no longer equal to x .¹³ Also, the plateau in $R_H(T)$ at moderate temperature observed in the lightly-doped region is now replaced by a peaked temperature dependence, which points to the necessity of an elaborate model to understand its behavior at low to moderate temperature. Nevertheless, as is obvious in Fig. 1, in those samples the behavior of $R_H(T)$ at high temperature is surprisingly similar to that observed in lightly-doped samples and is changing only gradually with doping; this observation strongly suggests that essentially the same thermal activation process is affecting the $R_H(T)$ behavior at high temperature even in the superconducting dop-

ing range. Motivated by this qualitative observation, we attempt to understand the high-temperature $R_H(T)$ behavior for $x \geq 0.08$ in terms of a crude phenomenological two-carrier model, remembering that the occurrence of an electronic heterogeneity (microscopic phase separation or coexistence of different types of carriers) has been discussed repeatedly for LSCO;^{6,34,35,36,37,38,39} for example, doping evolutions of the magnetic susceptibility³⁴ or the superfluid density³⁵ have been discussed to reflect an electronic heterogeneity. In the following analysis, we crudely hypothesize that there are two types of holes, those that live on the Fermi arc (or small hole pockets), and others that live on a large Fermi surface (FS). We suppose that the former contribute to the Hall effect with the component R_H^{arc} described by Eq. (2), while the latter contribute with a component $R_H^{LFS} = V_{Cu}/en_2$. For the sake of simplicity, we further suppose that these two components R_H^{arc} and R_H^{LFS} are additive in the expression of the total Hall coefficient with their respective fractions f and $1-f$, as is the case with the two-carrier model proposed for cuprates by Lee and Nagaosa.⁴⁰ Hence, we try to see how $R_H(T)$ at high temperature can be described in terms of the expression

$$R_H(T) = fR_H^{arc} + (1-f)R_H^{LFS} \quad (3)$$

$$= \frac{V_{Cu}}{e} \left[f/(x + n_1 e^{-\Delta_{CT}/2k_B T}) + (1-f)/n_2 \right]. \quad (4)$$

We emphasize that Eq. (4) should be considered to be essentially a working hypothesis that is not backed by a concrete theory, and this expression naturally fails at low to moderate temperature where R_H shows a non-trivial temperature dependence due, for example, to the scattering-time anisotropy.^{9,41} Actually, already in the upper end of the lightly-doped region discussed in the previous subsection (i.e., $x = 0.04$ and 0.05), a slight deviation of the data from the fitting is evident below 300 K in Fig. 3(a), which is likely to be due to the intrinsic temperature dependence of R_H in the coherent regime.

The solid lines in Figs. 4(a)-4(e) show the fits of the data for $x = 0.08 - 0.21$ to Eq. (4). It is rather surprising that our crude model very well describes the experimental data for $T > 300$ K. As is noted above, it is expected from the beginning that Eq. (4) does not fit the data at low to moderate temperature, but intriguingly the value of R_H in the plateau region of our fit turned out to bear reasonable physical meaning. Remember, it has been known from the pulsed high-magnetic-field experiments^{1,42,43} that the normal-state Hall coefficient in the $T \rightarrow 0$ limit, $R_H(0)$, which is expected to genuinely reflect the electronic structure,⁴¹ is much smaller than that at T_c . We plot $R_H(0)$ obtained from recent measurements⁴³ of LSCO with squares in Figs. 4(a)-4(e), which agree reasonably well with what our fittings would suggest.⁴⁴ This gives phenomenological support to the validity of Eq. (4), and implies that the evolution of the effective carrier density at low temperature, which would be directly reflected in the measured R_H for $T \rightarrow 0$, may be understood in the framework of a two-carrier model

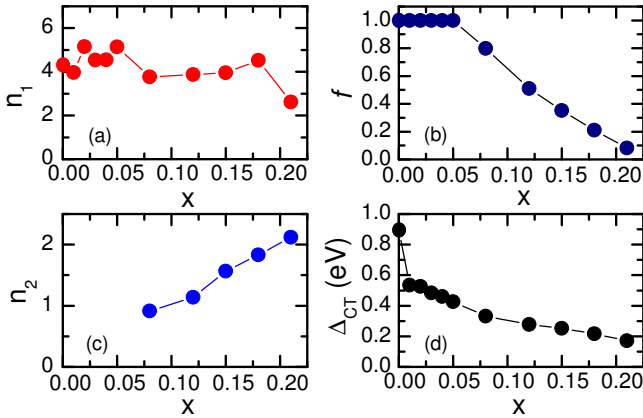


FIG. 5: (color online) Doping dependences of the fitting parameters for $R_H(T)$ of LSCO. (a) n_1 , a rough measure of the number of available states in the bands relevant to the thermal activation in the component R_H^{arc} which is presumably associated with the Fermi arc; (b) f , fraction of the component R_H^{arc} ; (c) n_2 , effective hole number in the component R_H^{LFS} presumably associated with a large Fermi surface; (d) Δ_{CT} , energy gap for the thermal activation.

in LSCO. The apparent success of our crude model in describing the R_H values at both high temperature and at 0 K at the same time seems to suggest that there is a certain truth in the above approach and calls for theoretical attentions.

The doping dependences of the fitting parameters are shown in Fig. 5, in which the results for the parent insulator and the lightly-doped samples discussed in the previous subsections are combined. It is notable that n_1 is essentially doping-independent up to $x = 0.18$ [Fig. 5(a)], which suggests that the physical origin of the thermally activated contribution is essentially unchanged up to optimum doping. On the other hand, the fraction f for the component R_H^{arc} , only in which the thermal activation is relevant, decreases rapidly for $x > 0.05$ [Fig. 5(b)], which causes the overall temperature dependence in R_H to become weaker as the overdoped region is approached. The parameter n_2 , the effective hole number associated with the large FS, is of the order of 1 as expected [Fig. 5(c)], and its doping dependence is likely to reflect the change in the FS shape observed by angle-resolved photo-emission spectroscopy (ARPES) experiments;¹² namely, as the shape of the large FS changes from hole-like to electron-like upon overdoping, R_H^{LFS} is expected to present a sign change, and hence n_2 ($= V_{Cu}/eR_H^{LFS}$) should eventually diverge.

To demonstrate the quality of our analysis, we show in Fig. 6 the Arrhenius plot of the activation term $n_{act} [= (n_1/f)e^{-\Delta_{CT}/2k_B T}]$, which is obtained from the R_H data after subtracting the constant contribution from the R_H^{LFS} component and that from the x -number of holes in the R_H^{arc} component; namely, after determining all the parameters of Eq. (4),⁴⁴ we obtain n_{act} by calculating $[eR_H/V_{Cu} - (1-f)/n_2]^{-1} - (x/f)$. Remember, the

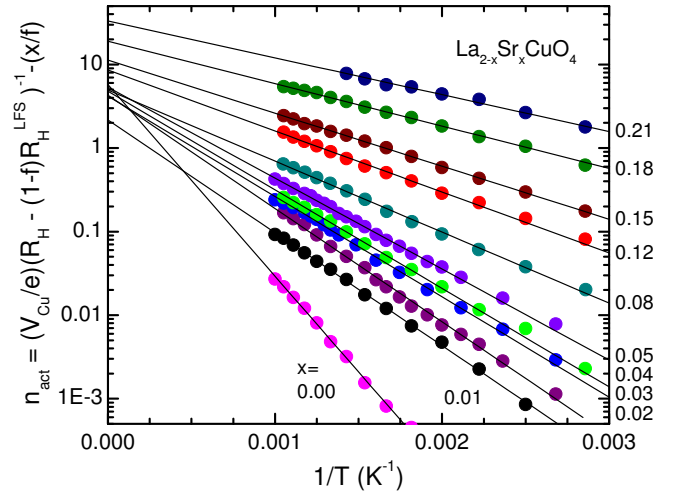


FIG. 6: (color online) Arrhenius plot of the activation term n_{act} , obtained from the R_H data by subtracting the constant contributions, for all x values. The solid lines are straight-line fits to the data to emphasize the activated behavior.

constant contributions used for calculating n_{act} from the raw R_H data are justified by the reasonable agreement between $R_H(0)$ and our fits for $T \rightarrow 0$. Figure 6 clearly testifies that the T -dependence of R_H above ~ 300 K is of activated nature.

As discussed in Sec. III-B, the gap Δ_{CT} for the thermal activation [Fig. 5(d)] shows a sudden drop from $x = 0$ to 0.01 and then shows only a small decrease with x in the lightly-doped region where our analysis for obtaining Δ_{CT} is robust. This weak doping dependence of Δ_{CT} appears to continue into the superconducting doping range, although one should take this result with a grain of salt, given the crude nature of our analysis for this region. Nevertheless, it is probably reasonable to conclude from our analysis that there remain charge fluctuations associated with some charge-transfer excitations deep into the superconducting doping region, and such fluctuations keep causing a thermally-activated temperature dependence in R_H at high temperature.

IV. DISCUSSIONS

The doping dependence of f shown in Fig. 5(b) suggests that the crossover in dominance from the Fermi arc to the large FS is pivoted at $x = 0.08$, and intriguingly this crossover around $x = 0.08$ appears to be reflected in a qualitative change in the temperature dependence of the in-plane resistivity ρ_{ab} . This situation is most easily seen in the plot of $x\rho_{ab}$ vs. T up to 1000 K shown in Fig. 7; here, the data for $x = 0.01 - 0.05$ show a clear tendency towards saturation at high temperature, which presumably comes from the increasing number of thermally-created holes, whereas such a tendency is mostly absent in the data for $x = 0.12 - 0.18$ where

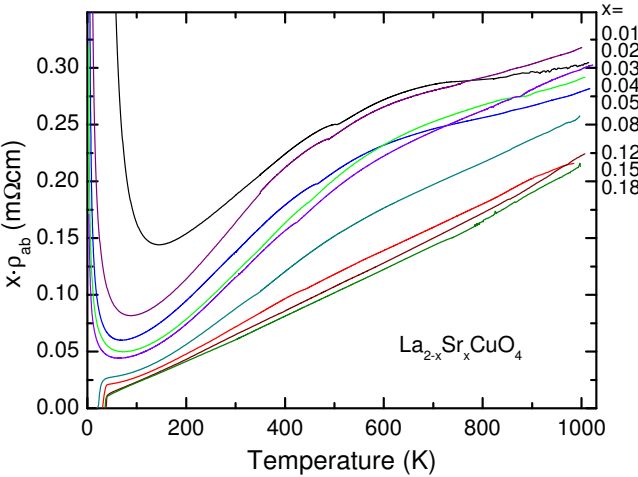


FIG. 7: (color online) T -dependences of the product $x\rho_{ab}$ for $x = 0.01 - 0.18$ up to 1000 K; note that x is a non-dimensional parameter.

the thermal activation occurs only in the minority component. It is useful to note that, within our model, the contribution from R_H^{arc} to the total R_H remain relatively large at low temperature even when f is small because of the smallness of x compared to n_2 [note that R_H at low temperature is written as $(V_{Cu}/e)\{f/x + (1-f)/n_2\}$; for example, even though f is only 0.2 at $x = 0.18$, roughly 2/3 of the total R_H is due to the component R_H^{arc} at low temperature, which is responsible for the 60% decrease in the total R_H from 200 to 950 K. Hence, it is possible that ρ_{ab} is insensitive to what is happening in the minority component, while R_H is more sensitive to the thermal activations taking place in the minority component.

It is useful to mention that in cuprates there is a celebrated “scattering-time separation” of charge carriers (i.e., the T dependences of resistivity and cotangent of the Hall angle, $\cot\theta_H$, present different powers of T).⁶ In our data, $\cot\theta_H$ behaves as $\sim T^2$ only below ~ 400 K in the superconducting doping range (Fig. 8), which suggests that the deviation of R_H from the fittings shown in Figs. 4(a)-4(e) may be linked to the appearance of two scattering times. This is reasonable, because thermally-created carriers are incoherent and blur the scattering-time separation at high temperature; also, the scattering-time separation would disappear at low enough temperature where the elastic impurity scattering dominates, if it is due to a development of scattering-time anisotropy in the momentum space.^{9,41,45,46} Hence, our data seem to suggest that the scattering-time separation is a result of a peculiar scattering-time anisotropy,^{9,45,46} which develops only at intermediate temperature. In passing, similar scattering-time separations have been found in non-cuprate materials,^{2,4,47,48} suggesting that this phenomenon may not be very special.

It is worth emphasizing that the picture derived here (appearance of activated carriers at high temperature and growth of the contribution from a large FS in the su-

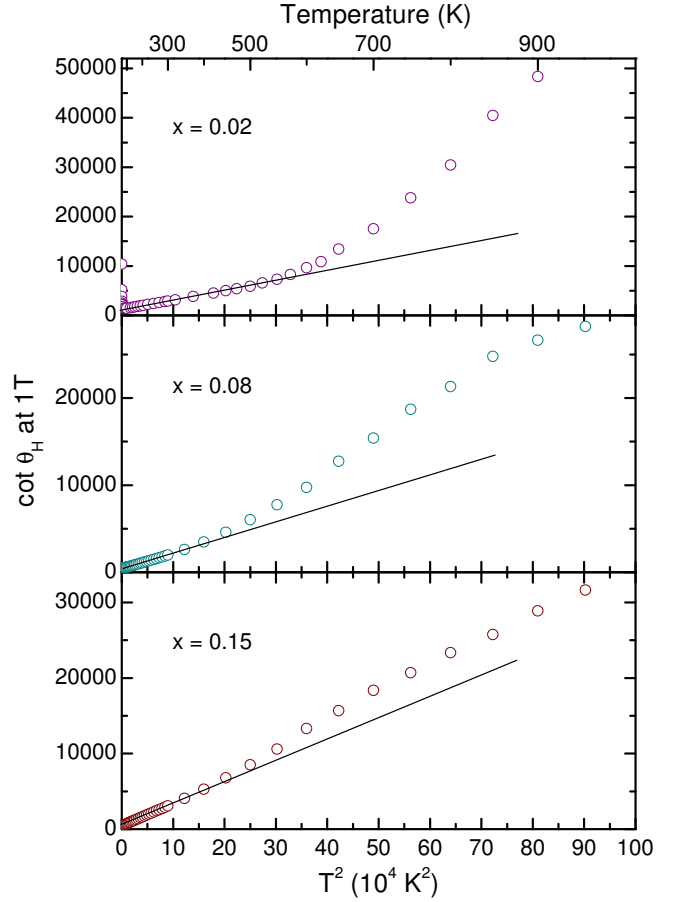


FIG. 8: (color online) Plots of $\cot\theta_H$ (at 1 T) vs T^2 for three representative dopings. The solid lines emphasize the T^2 law that holds at low temperature.

perconducting doping range) not only explains the Hall effect but also is consistent with the resistivity data, as can be inferred in Fig. 7. Also, the magnetic susceptibility data up to 800 K (Ref. 49) have been analyzed³⁴ with a similar model and are essentially consistent with our conclusion. In view of the present picture, we can probably address some of the complications regarding the pseudogap.⁶ In the past, a scaling of $R_H(T)$ was used²² to identify a characteristic temperature T^* that reaches ~ 700 K at low doping, and this T^* was shown to agree with those deduced from the dc magnetic susceptibility or the Knight shift. Since this T^* is much higher than the pseudogap temperature deduced from spectroscopic means,⁶ it is often called “large pseudogap”. Our results imply that the large pseudogap is related to the freezing of the thermal creation of charge carriers, which causes the chemical potential to move and thereby affects various physical quantities.

V. CONCLUSION

We have shown that the behavior of $R_H(T)$ in insulating LSCO ($x = 0 - 0.05$) at high temperature clearly signifies that charge carriers are thermally activated over a sub-eV gap, likely associated with some charge-transfer excitations. In the superconducting doping region, the high-temperature $R_H(T)$ behavior is found to be qualitatively the same but is weakened, which we try to describe with a phenomenological two-carrier model that considers the thermal activation for one of the two components. Besides giving a perspective to consistently understand the high-temperature behavior of R_H and ρ_{ab} , our model allows us to understand the R_H value both at high temperature and at 0 K for a wide range of doping, despite its crudeness. Overall, our data and analysis strongly suggest that charge fluctuations associated with a sub-eV gap should be taken into account when discussing the physics of cuprates even at relatively low energy scales.

Implications of this conclusion include: (1) breakdown of the T^2 law of $\cot \theta_H$ at high temperature may be related to the onset of incoherence in one of the two species of the carriers, that dominates the Hall effect but little influences the resistivity near optimum doping; (2) “opening of the large pseudogap” may actually be a “freezing of charge fluctuations” associated with the Fermi arc.

Acknowledgments

We greatly thank L. P. Gor'kov and G. B. Teitelbaum for illuminating discussions and pointing out an activated behavior in our data. We also thank E. Abrahams, B. Batlogg, T. H. Geballe, J. Fink, S. A. Kivelson, P. B. Littlewood, N. P. Ong, D. Pines, G. A. Sawatzky, X. F. Sun, A. A. Taskin, T. Tohyama, I. Tsukada, and S. Uchida for helpful discussions. This work was supported by Grant-in-Aid for Science from JSPS.

* Corresponding author. e-mail: ando@criepi.denken.or.jp
¹ F. F. Balakirev *et al.*, Nature **424**, 912 (2003).
² S. Paschen *et al.*, Nature **432**, 881 (2004).
³ Y. Dagan, M. M. Qazilbash, C. P. Hill, V. N. Kulkarni, and R. L. Greene, Phys. Rev. Lett. **92**, 167001 (2004).
⁴ A. Yeh *et al.*, Nature **419**, 459 (2002).
⁵ T. Noda, H. Eisaki, and S. Uchida, Science **286**, 265 (1999).
⁶ J. Orenstein and A. Millis, Science **288**, 468 (2000).
⁷ S. A. Kivelson *et al.*, Rev. Mod. Phys. **75**, 1201 (2003).
⁸ P. W. Anderson, Phys. Rev. Lett. **67**, 2092 (1991).
⁹ B. P. Stojkovic and D. Pines, Phys. Rev. B **55**, 8576 (1997).
¹⁰ H. Kontani, K. Kanki, and K. Ueda, Phys. Rev. B **59**, 14723 (1999).
¹¹ D. Veberic and P. Prelovsek, Phys. Rev. B **66**, 020408(R) (1999).
¹² A. Damascelli, Z. Hussain, and Z.-X. Shen, Rev. Mod. Phys. **75**, 473 (2003).
¹³ Y. Ando, Y. Kurita, S. Komiya, S. Ono, and K. Segawa, Phys. Rev. Lett. **92**, 197001 (2004).
¹⁴ M. A. Kastner, R. J. Birgeneau, G. Shirane, and Y. Endoh, Rev. Mod. Phys. **70**, 897 (1998).
¹⁵ E. Dagotto, Rev. Mod. Phys. **66**, 763 (1994).
¹⁶ T. H. Geballe and B. Y. Moyzhes, Ann. Phys. (Leipzig) **13**, 20 (2004).
¹⁷ S. Komiya, Y. Ando, X. F. Sun, and A. N. Lavrov, Phys. Rev. B **65**, 214535 (2002).
¹⁸ S. Komiya, H.-D. Chen, S.-C. Zhang, and Y. Ando, Phys. Rev. Lett. **94**, 207004 (2005).
¹⁹ A. A. Taskin, A. N. Lavrov, and Y. Ando, Appl. Phys. Lett. **86**, 091910 (2005).
²⁰ H. Kanai *et al.*, J. Solid State Chem. **131**, 150 (1997).
²¹ T. Nishikawa, J. Takeda, and M. Sato, J. Phys. Soc. Jpn. **63**, 1441 (1994).
²² H. Y. Hwang *et al.*, Phys. Rev. Lett. **72**, 2636 (1994).
²³ The binding energy of the holes to the oxygen acceptor mentioned in Ref. 14 is the activation energy obtained from the Arrhenius plot, which corresponds to 1/2 of Δ_{imp} de-

fined in Eq. (1). (This is because the chemical potential moves to the middle of the gap when the thermal activation process becomes dominant). Hence, our result of $\Delta_{imp} = 87$ meV is essentially consistent with Ref. 14 where the binding energy was mentioned to be 35 meV.
²⁴ D. Adler and J. Feinleib, Phys. Rev. B **2**, 3112 (1970).
²⁵ Remember that in an intrinsic semiconductor the Hall coefficient is given by $R_H = (\mu_h - \mu_e)/[ne(\mu_h + \mu_e)]$, where μ_h (μ_e) is the mobility of holes (electrons) and $n = n_1 e^{-\Delta/2k_B T}$ is the number of pair-created electrons and holes. Hence, the effective density of states is always enhanced by the factor $(\mu_h + \mu_e)/|\mu_h - \mu_e|$.
²⁶ R. S. Markiewicz and A. Bansil, Phys. Rev. Lett. **96**, 107005 (2006).
²⁷ K. M. Shen *et al.*, Phys. Rev. Lett. **93**, 267002 (2004).
²⁸ In those fittings, x was actually treated as a fitting parameter, because there is an uncertainty of up to 10% in the compositional x values in lightly-doped samples. The resulting x values obtained from the fits are 0.0098, 0.0213, 0.0369, 0.0440, and 0.0546 for the five sets of data, all in reasonable agreement with the compositional values.
²⁹ M. B. J. Meinders, H. Eskes, and G. A. Sawatzky, Phys. Rev. B **48**, 3916 (1993).
³⁰ In conventional semiconductor physics, n_1 is actually a temperature-dependent effective density of states that is viewed to be concentrated at the band edge, and its value is determined largely by the shape of the actual density of states near the edge. The temperature dependence of n_1 (which, for example, is $T^{2/3}$ in the case of a parabolic band in a 3D system) is often neglected because it is much weaker than the exponential term.
³¹ W. J. Padilla, Y. S. Lee, M. Dumm, G. Blumberg, S. Ono, K. Segawa, S. Komiya, Y. Ando, and D. N. Basov, Phys. Rev. B **72**, 060511(R) (2005).
³² J. Fink *et al.*, J. Electron Spectroscopy and Related Phenomena **66**, 395 (1994).
³³ Y.-J. Kim *et al.*, Phys. Rev. B **70**, 094524 (2004).
³⁴ K. A. Müller, Physica C **341-348**, 11 (2000).

³⁵ Y. J. Uemura, Solid State Commun. **120**, 347 (2001).

³⁶ L. P. Gor'kov, J. Supercond. **14**, 365 (2001).

³⁷ M. Mayr, G. Alvarez, A. Moreo, and E. Dagotto, Phys. Rev. B **73**, 014509 (2006).

³⁸ S. A. Kivelson, E. Fradkin, and T. H. Geballe, Phys. Rev. B **69**, 144505 (2004).

³⁹ J. M. Tranquada, Proc. SPIE **5932**, 59320C (2005).

⁴⁰ P. A. Lee and N. Nagaosa, Phys. Rev. B **46**, 5621 (1992).

⁴¹ N. P. Ong, Phys. Rev. B **43**, 193-201 (1991).

⁴² Y. Ando *et al.*, Phys. Rev. B **56**, R8530 (1997).

⁴³ F. F. Balakirev, J. B. Betts, A. Migliori, G. S. Boebinger, I. Tsukada, and Y. Ando, NHMFL 2005 Annual Report.

⁴⁴ In our fitting procedure, the parameters are determined so that the widest range of the high-temperature data are fitted to the exponential behavior. Hence, the temperature below which the fitting fails and the the plateau value of our fit come out naturally without any subjective choice in the procedure.

⁴⁵ L. B. Ioffe and A. J. Millis, Phys. Rev. B **58**, 11631 (1998).

⁴⁶ N. E. Hussey, Eur. Phys. J. B **31**, 495 (2003).

⁴⁷ Y. Nakajima *et al.*, J. Phys. Soc. Jpn. **73**, 5 (2004).

⁴⁸ T. F. Rosenbaum, A. Husmann, S. A. Carter, and J. M. Honig, Phys. Rev. B **57**, R13997 (1998).

⁴⁹ D. C. Johnston, Phys. Rev. Lett. **62**, 957 (1989).